PRESSURE ANALYSIS OF DAM-BREAK AND WAVE-BREAKING BY SPH MODEL

Songdong SHAO[1] and Hitoshi GOTOH[2]

[1]Member of JSCE, Dr. Eng., JSPS Postdoctoral Fellow, Dept. of Civil Eng., Kyoto University
(Yoshida Hon-machi, Sakyo-ku, Kyoto, 606-8501, Japan)
[2]Member of JSCE, Dr. Eng., Associate Professor, Dept. of Civil Eng., Kyoto University

The Smoothed Particle Hydrodynamics (SPH) method is put forward to simulate dam-break and wave-breaking problem. The Lagrangian form of governing equations are solved by a two-step split scheme and the basic SPH formulations are employed to discretize the gradient and divergence operators in the equations. The SPH model is robust for tracking free surfaces by particles without numerical diffusion. The pressure characteristics are analyzed based on computations. It is shown that the dynamic pressure is very strong in the early stage of dam-break and wave-breaking but quickly settles down in the later stages.

Key Words: *SPH, dynamic pressure, dam-break, wave-breaking*

1. INTRODUCTION

Free surface hydrodynamic flows are of industrial and environmental importance but they are difficult to simulate because the surface boundary conditions are specified on an arbitrarily moving surface. The MAC[1)] and VOF[2)] methods are two of the most flexible and robust approaches for treating such flows. However, in both the MAC and VOF methods, the Navier-Stokes equations are solved on a fixed Eulerian grid. Problems of numerical diffusion arise due to advection terms in the N-S equations and the numerical diffusion becomes severe when the deformation of the free surface is very large.

The smoothed particle hydrodynamics (SPH) is a pure Lagrangian method originally developed for astrophysical computations[3)] and has later been extended to model a wide range of hydrodynamic problems. The basic concept of SPH is that a particle is fundamental in the Lagrangian description and the motion of a continuum can be represented with arbitrary accuracy by simulating the advection of a large number of such particles. Through the use of integral interpolants, the dependent field variables are expressed by integrals which are approximated by summation interpolants over neighboring particles. Thus each term in the N-S equations can be represented by SPH formulation. Incorporated with initial and boundary conditions, the whole equations are solvable. The incompressibility of the fluid is satisfied by keeping the particle density equal to its initial value through a pressure Poisson equation.

In this paper a SPH model based on MPS solver[4),5)] is applied to dam-break and wave-breaking problems. The initial SPH scheme is fully explicit. When dealing with fluid flows, incompressibility was realized through an equation of state so that the fluid is assumed to be weakly compressible. In this case, a large sound speed has to be introduced, which could easily cause problems of sound wave reflection at the boundary and lead to computational instability. In this paper, a real incompressible SPH model is proposed based on MPS solver in that the pressure is not a thermodynamic variable obtained from the equation of state, but rather by way of solving a pressure Poisson equation derived from a semi-implicit algorithm of pressure projection. Thus both computational efficiency and stability have been greatly improved. Another advantage of the proposed SPH model lies in that it can obtain highly stable pressure fields. Many other Lagrangian approaches, including the MPS method, are not free from the stochastic behavior of calculating points or particles, which also brings the fluctuation of the

pressure. However, SPH formulations employ analytical kernel to represent integration, as well as gradient and divergence with higher resolution, superior to the corresponding MPS interaction models. Thus SPH method will provide a useful tool to analyze dynamic pressure properties for the Benchmark problems.

2. GOVERNING EQUATIONS

The governing equations for SPH model are the mass and momentum conservation equations written in Lagrange form as

$$\frac{1}{\rho}\frac{D\rho}{Dt}+\nabla\cdot\mathbf{u}=0 \tag{1}$$

$$\frac{D\mathbf{u}}{Dt}=-\frac{1}{\rho}\nabla P+\mathbf{g}+\nu\nabla^2\mathbf{u} \tag{2}$$

where ρ = fluid density; t = time; $\mathbf{u}$ = velocity; P = pressure; $\mathbf{g}$ = gravitational acceleration and ν = kinematic viscosity.

The SPH computation consists of two steps, i.e. prediction and correction, similar to those employed in the MPS[4),5)] method. The prediction step is an explicit integration in the time domain without enforcing incompressibility. Only the viscous and gravitational terms in the Navier-Stokes equation (2) are used and an intermediate particle velocity and position are obtained. At this moment the incompressibility is not satisfied, which is reflected by that the particle density deviates from the initial values. Thus a second corrective step is applied to adjust fluid densities at the particles to initial values prior to the time step. In the correction, the pressure term is used to update the particle velocity obtained from the intermediate step. The pressure for enforcing incompressibility is derived from the mass conservation Equation (1) and obtained by solving a pressure Poisson equation. The relevant processes are summarized as follows:

Prediction

$$\mathbf{u}_*=\mathbf{u}_t+\Delta\mathbf{u}_* \tag{3}$$

$$\Delta\mathbf{u}_*=(\mathbf{g}+\nu\nabla^2\mathbf{u})\Delta t \tag{4}$$

$$\mathbf{r}_*=\mathbf{r}_t+\mathbf{u}_*\Delta t \tag{5}$$

where $\mathbf{u}_t$ and $\mathbf{r}_t$ = particle velocity and position at time t; $\mathbf{u}_*$ and $\mathbf{r}_*$ = intermediate particle velocity and position; $\Delta\mathbf{u}_*$ = changed particle velocity during the prediction step and Δt = time increment.

Correction

$$\Delta\mathbf{u}_{**}=-\frac{1}{\rho_*}\nabla P_{t+1}\Delta t \tag{6}$$

$$\mathbf{u}_{t+1}=\mathbf{u}_*+\Delta\mathbf{u}_{**} \tag{7}$$

$$\mathbf{r}_{t+1}=\mathbf{r}_t+\frac{(\mathbf{u}_t+\mathbf{u}_{t+1})}{2}\Delta t \tag{8}$$

where $\Delta\mathbf{u}_{**}$ = changed particle velocity during the correction step; ρ_* = intermediate particle density between the prediction and correction; P_{t+1} and $\mathbf{u}_{t+1}$ = particle pressure and velocity of time $t+1$; and $\mathbf{r}_t$ and $\mathbf{r}_{t+1}$ = positions of particle in time t and $t+1$.

Pressure Equation

$$\nabla\cdot(\frac{1}{\rho_*}\nabla P_{t+1})=\frac{\rho_0-\rho_*}{\rho_0\Delta t^2} \tag{9}$$

where ρ_0 = initial constant density at each of the particles. This equation is analogous to the formulation in the MPS method in that the source term of the Poisson equation is the variation of particle densities, while it is usually the divergence of intermediate velocity vector in finite difference methods.

3. SPH FORMULATIONS

The SPH formulations are employed to represent the summation, gradient, divergence and viscosity (Laplacian) of all particles in the governing equations. Each particle carries a mass m, velocity $\mathbf{u}$ and other properties, depending on the problem.

The fluid density at particle a, ρ_a is evaluated by

$$\rho_a=\sum_b m_b W(|\mathbf{r}_a-\mathbf{r}_b|,h) \tag{10}$$

where a and b = reference particle and its neighbors; $\mathbf{r}_a$ and $\mathbf{r}_b$ = position of particles; and W = interpolation kernel and h = smoothing distance, which is set twice the initial particle spacing in the computation. Kernels W can assume many different forms and the use of different kernels is the SPH analogue of using various difference schemes in finite difference methods. The kernel can be differentiated analytically without the use of grids. If the grids are fixed in position the SPH equations are identical to finite difference equations with different forms depending on the interpolation kernel. By

balancing the computational accuracy and efficiency, the kernel based on the spline function and normalized in 2-D is adopted in this paper[3].

The gradient of the pressure is expressed as

$$(\frac{1}{\rho}\nabla P)_a = \sum_b m_b(\frac{P_a}{\rho_a^2}+\frac{P_b}{\rho_b^2})\nabla_a W_{ab} \quad (11)$$

where the summation is over all particles other than particle a and $\nabla_a W_{ab}$ = gradient of the kernel taken with respect to the positions of particle a. Similarly, the divergence of a vector $\mathbf{u}$ at particle a can be formulated symmetrically by

$$\nabla\cdot\mathbf{u}_a = \rho_a\sum_b m_b(\frac{\mathbf{u}_a}{\rho_a^2}+\frac{\mathbf{u}_b}{\rho_b^2})\cdot\nabla_a W_{ab} \quad (12)$$

The Laplacian is formulated as a hybrid of a standard SPH first derivative with a finite difference approximation for the first derivative as

$$\nabla\cdot(\frac{1}{\rho}\nabla P)_a = \sum_b m_b\frac{8}{(\rho_a+\rho_b)^2}\frac{P_{ab}\mathbf{r}_{ab}\cdot\nabla_a W_{ab}}{|\mathbf{r}_{ab}|^2} \quad (13)$$

where $P_{ab}=P_a-P_b$ and $\mathbf{r}_{ab}=\mathbf{r}_a-\mathbf{r}_b$.

The viscosity term is formulated by

$$(\nu\nabla^2\mathbf{u})_a = \sum_b\frac{4m_b(\mu_a+\mu_b)\mathbf{r}_{ab}\cdot\nabla_a W_{ab}}{(\rho_a+\rho_b)^2|\mathbf{r}_{ab}|^2}(\mathbf{u}_a-\mathbf{u}_b) \quad (14)$$

where $\mu=\rho\nu$ is dynamic viscosity.

4. FREE SURFACE TREATMENT

In SPH model free surfaces can be easily identified by particle densities. Since no particle exists above the free surface, the particle density will decrease on the surface. A particle is regarded as a surface particle if its density fluctuation is over 1% below that of the inner fluid. A Dirichlet boundary condition of zero pressure is given to this particle. Unlike wall particles which are also calculated in the pressure Poisson equation, there is no such a need for these surface particles.

5. DAM-BREAK COMPUTATIONS

Dam-break flows are an important practical problem in the civil engineering and their prediction is now a required element in the design of a dam and its surrounding environment. In this example, one rectangular column of water in hydrostatic equilibrium is confined between two vertical walls. The water column is 1 unites wide and 2 unites high and gravity is acting downward with unit magnitude. At the beginning of the computation, the right wall (dam) is instantaneously removed and the water is allowed to flow out along a dry horizontal bed. Experimental data[6] are available for validation against the SPH calculations. At beginning the SPH fluid particles are initially arranged in a regular, equally-spaced grid, with boundary particles added to form the left-hand wall and bed. In the simulation the time step Δt is continuously adjusted for computational efficiency based on the Courant constraint, i.e., the maximum particle displacement during one time step should be smaller than a part of initial particle spacing. In order to account for the influence of the turbulence, the viscosity in simulation is taken to be 1000 times larger than that of the constant laminar value, i.e., $\nu = 10^{-3}$ m^2/s. Totally 5000 SPH particles are involved in the computations.

Fig. 1 shows the comparison of the time variation of the leading edge from the left wall with experiments from Martin and Moyce[6]. The relations between the normalized time $T=t(g/a)^{1/2}$ (where a is initial dam height) and leading edge $X=x/a$ are in good agreement, validating the accuracy of the SPH.

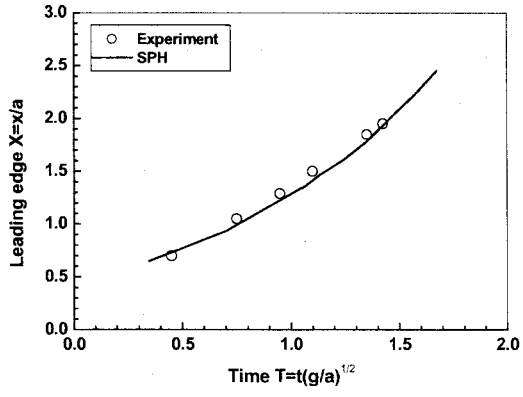

Fig. 1 Experimental and numerical leading edge against time of dam-break flow

In order to further demonstrate the robustness of the SPH, the time sequences of instantaneous particle snapshots, total pressure and dynamic pressure contours are given in three columns in Fig.2 (a), (b) and (c), respectively. In the figure the length scale has been normalized by a, the time scale by $1/(g/a)^{1/2}$ and the pressure scale by $\rho g a$. It is seen from the particle snapshots in the first column that

SPH can well reproduce the formation of a bore in the flow front near the bottom, which is due to the advantage that the SPH can clearly describe the free surfaces without numerical diffusion. From the total pressure contours in the second column of Fig. 2, it is shown that at the early stage of the dam-break flow at time $t(g/a)^{1/2} = 0.35$, the pressure distribution inside the fluid deviates significantly from hydrostatic and the maximum pressure is only half of the hydrostatic value. This is due to the large downwards particle acceleration after the sudden release of the right dam. As time goes on, the initial large acceleration decreases and the pressure gradually becomes uniform, until a bore develops downstream as seen from time $t(g/a)^{1/2} = 0.7$ to 1.05. Meanwhile, the magnitude of the pressure also gradually increases until the pressure distribution is almost hydrostatic. The above pressure development patterns have also been reported in other literatures[7]. Further examining the dynamic pressure distributions in the third column of Fig. 2, it is much more clear that the dynamic pressure is very strong and globally distributed in the whole flow domain at the early stages of dam-break. Also with time elapsing on, the dynamic pressure becomes locally concentrated near the initial dam-site and the amplitude of the negative pressure is only 15% of its maximum value.

Thus, a useful conclusion can be drawn for practical purposes from this point. The shallow water equation, which is based on the hydrostatic assumption and uniform velocity over the depth, is only applicable at the later stages of the dam-break flow when a bore fully develops downstream. It will cause significant errors if applied at the very early stage of dam-break.

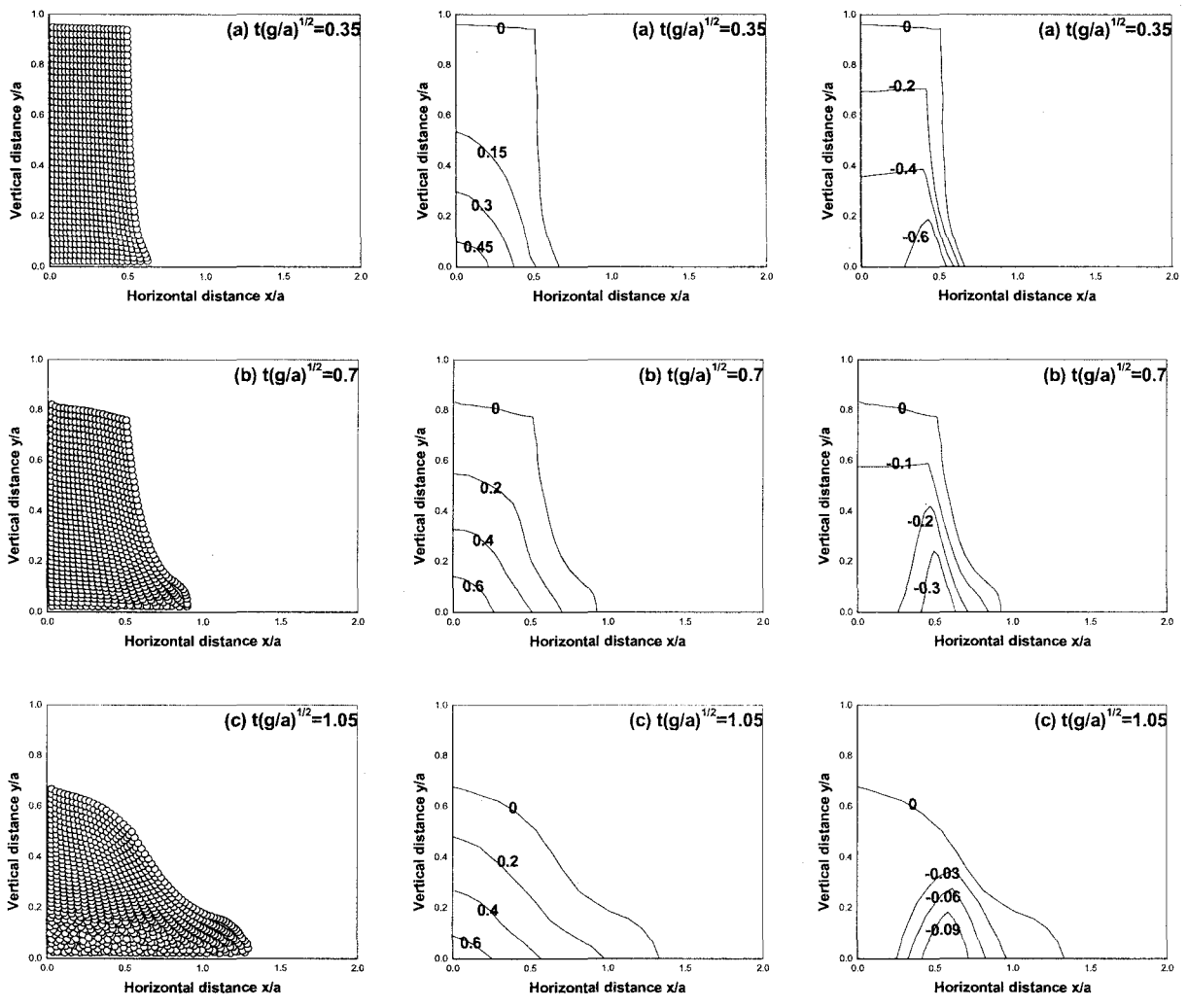

Fig. 2 Time sequences of particle snapshots (first column), total pressure (second column) and dynamic pressure (third column) at time $t(g/a)^{1/2}$ (a) 0.35; (b) 0.7; and (c) 1.05, respectively

6. WAVE-BREAKING COMPUTATIONS

The solitary wave-breaking near the beach is also an important practical problem relevant to tsunami hazard mitigation in coastal regions. In this section, the laboratory breaking solitary wave data of Synolakis[8] is used as another good test for the SPH model. The wave broke and ran up on a mild 1:20 slope. SPH simulation reproduces the experiment in which the still water depth was d = 0.21 m and the incident wave height H/d was 0.28. Approximately 10000 particles are employed in the computation. The time step is also automatically adjusted during the computation to achieve efficiency and the viscosity ν is taken to be 10^{-3} m^2/s during the wave breaking and 10^{-4} m^2/s during the subsequent runup processes. The computed time sequences of instantaneous particle snapshots, total pressure and dynamic pressure contours are given in three columns in Fig. 3 (a), (b) and (c), respectively. Also in the figure the length, time and pressure scales have been normalized as in the dam-break computations and only the upper part of the flow over the slope is plotted. In the second column of Fig. 3, the experimental data of surface profiles are given for comparison with the SPH computations. It is seen that the general agreement between the two is satisfactory, further verifying the accuracy of SPH.

The SPH particle snapshots in the first column in Fig. 3 clearly reproduce the time sequences of wave-breaking, turbulence bore formation and running up a slope. In the second column, it is shown that when the wave breaks at time $t(g/d)^{1/2} = 20$, the pressure in the still water in front of the breaking front deviates significantly from hydrostatic and is about two times that of the hydrostatic value.

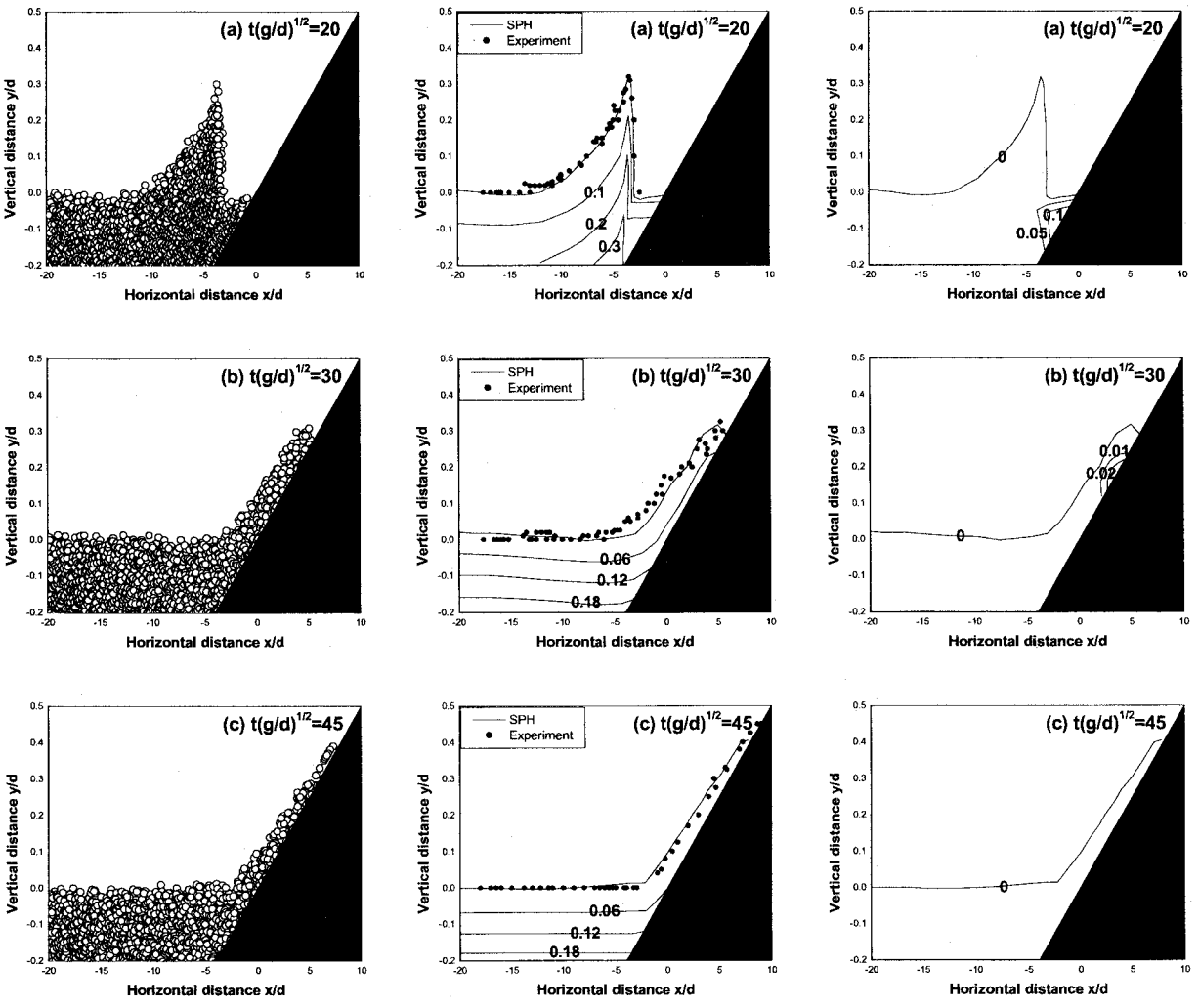

Fig. 3 Time sequences of particle snapshots (first column), total pressure (second column) and dynamic pressure (third column) at time $t(g/d)^{1/2}$ (a) 20; (b) 30; and (c) 45, respectively. Experiemtal data are given in the second column

This is due to the reason that the fluid particles in the still water in front of the moving bore are undergoing the processes of being static to moving forward and upward. Thus the vertical acceleration of particles is always positive, which increases the pressure there.

However, during the subsequent bore running up from $t(g/d)^{1/2} = 30$ to 45, the pressure returns back to be hydrostatic everywhere. The same findings have also been reported by Lin et al.[9] in his VOF simulation of solitary wave breaking using Reynolds-averaged N-S equations. The dynamic pressures in the third column of Fig. 3 describe this phenomena more clearly in that during the wave-breaking, the maximum positive dynamic pressure is almost equivalent of the hydrostatic one, but it decreases rapidly and totally disappears during the subsequent running up. Thus another useful conclusion can be drawn from the computations. The shallow water equation, which assumes hydrostatic distribution and has been widely applied to study coastal wave mechanics, is accurate enough for analyzing wave propagating, shoaling as well as later running up processes, etc. It is only inapplicable within a narrow region in front of breaking front, where the influence of dynamic pressures is too strong to be neglected.

7. CONCLUSIONS AND SUMMARY

The paper presents a SPH particle model to study the dynamic pressure characteristics in dam-break and wave-breaking. The model is effective in tracking free surfaces by particles. It is shown that during the early stages of dam-break and wave-breaking, the pressure deviates significantly from hydrostatic and the dynamic pressure is the same magnitude as the hydrostatic value. However, the pressure distributions recover to almost be hydrostatic during the later stages of dam-break and wave-breaking after the formation of a turbulence bore. This verifies that the widely used shallow-water equations can be applied to analyze such problems with enough accuracy.

Finally it should be noted that the computed pressures are quite stable in the above two SPH simulations. However, many other particle methods have the reported problems of pressure instability, since the pressure is calculated based on particle information and sensitive to particle positions and disorder. In comparison, relatively stable pressures have been obtained by SPH. This is due to that SPH uses analytical kernel to represent integration, as well as gradient and divergence in the governing N-S equations. The numerical results can better approximate exact solutions of the relevant problem if large numbers of particles are employed. Thus the computed field variables are much more smoothed and stable than those obtained by other particle approaches.

ACKNOWLEDGEMENT: This research work was supported by the Japan Society for the Promotion of Science. We are also very grateful to Professor Tetsuo Sakai, Department of Civil Engineering, Kyoto University, for his valuable comments and suggestions on this work.

REFERENCES

1) Harlow, F. H. and Welch, J. E.: Numerical calculation of time-dependent viscous incompressible flow of fluid with free surface, Phys. Fluids, Vol. 8, No. 12, pp. 322-329, 1965.
2) Hirt, C. W. and Nichols, B. D.: Volume of fluid (VOF) method for the dynamics of free boundaries, J. Comp. Phys., Vol. 39, pp. 201-225, 1981.
3) Monaghan, J. J.: Smoothed particle hydrodynamics, Annu. Rev. Astron. Astrophys., Vol. 30, pp. 543-574, 1992.
4) Koshizuka S., Nobe, A. and Oka, Y.: Numerical analysis of breaking waves using the moving particle semi-implicit method, Int. J. Numer. Meth. Fluids, Vol. 26, pp. 751-769, 1998.
5) Gotoh, H. and Sakai, T.: Lagrangian simulation of breaking waves using particle method, Coastal Eng. J., JSCE, Vol. 41, No. 3&4, pp. 303-326, 1999.
6) Martin, J. C. and Moyce, W. J.: An experimental study of the collapse of liquid columns on a rigid horizontal plane, Philos. Trans. Roy. Soc. London Ser. A, Vol. 244, pp. 312-324, 1952.
7) Pan, C. H., Xu, X. Z. and Lin, B. Y.: Simulating free surface flows by MAC method, Estuarine and Coastal Eng., No. 1&2, pp. 51-58, 1993. (in Chinese)
8) Synolakis, C. E.: The run-up of long waves, Ph. D thesis, California Institute of Technology, Pasadena, California, pp. 228, 1986.
9) Lin, P. Z., Chang, K. A. and Liu Philip, L. F.: Runup and rundown of solitary waves on sloping beaches, J. Wtrwy. Port, Coast. and Oc. Eng., ASCE, Vol. 125, No. 5, pp. 247-255, 1999.

(Received September 30, 2002)